International Conference on Space Optics—ICSO 2018

Chania, Greece

9–12 October 2018

Edited by Zoran Sodnik, Nikos Karafolas, and Bruno Cugny

Radiation testing of optical coatings: better testing with simulations

Jochen Kuhnhenn

Michael Steffens

Max Baum

International Conference on Space Optics — ICSO 2018, edited by Zoran Sodnik, Nikos Karafolas, Bruno Cugny, Proc. of SPIE Vol. 11180, 111804L · © 2018 ESA and CNES · CCC code: 0277-786X/18/$18 · doi: 10.1117/12.2536084

Radiation Testing of Optical Coatings - Better Testing with Simulations

Jochen Kuhnhenn*, Michael Steffens, Max Baum
Fraunhofer INT, Appelsgarten 2, 53879 Euskirchen, Germany

ABSTRACT

Radiation testing of thin optical coatings for space requires different approaches compared to bulk optical components or other material samples. In contrast to thicker samples, already particles of lower energy and thus lower range in the material will deposit high levels of dose in functional areas. In this paper we will discuss those differences and show ways to develop optimized test strategies.

Keywords: Optical coatings, Radiation effects, Radiation testing, Numerical simulation, Thin films, Space environment

1. INTRODUCTION

Using optical components in presence of radiation is a challenge that differs from other harsh environments. While testing the influence of temperature, vacuum, or mechanical stress are usually well defined in standards, there is no common procedure to determine the influence of ionizing radiation on optics. Depending on the components and their function and the actual radiation conditions test procedures will be different and need adaption.

In space the radiation environment is defined by several contributions originating from the magnetic belts, the sun and outer space. Depending on the mission-orbit parameters, those contributions define the amount and energy distribution of the particles present. For nearly all of the effects and orbits, electrons and protons are the most abundant and thus important particles to consider. There exist several models to describe and calculate the particle flux as a function of time and orbit. Those models are limited with respect to covered energy and potential orbits. In applications those models are used to estimate the dose and fluence that a given component inside of the satellite should be targeted at.

Optical coatings, that are facing directly space and therefore are exposed without any shielding to the radiation, will suffer degradation that has to be qualified before the mission. In contrast to components inside of the satellite behind shielding, already particles of low energy will deposit their energy completely in the functional layers.

While there exist several standards that target parts of this topic, e.g. ISO 15856 [1], no practical approach has been developed to cover the individual aspects of different applications.

1.1 Radiation effects in optical coatings

The effects of space radiation, i.e. electrons and protons of varying energy, may induce several forms of degradation in thin optical coatings: sputtering could lead to change of surface roughness, ionizing dose darkens transparent media, displacement effects could change the interface composition between layers, or protons may induce hydrogen gas accumulation within the coating. This is especially important to consider for surfaces that are directly facing the space environment without any shielding.

In bulk optics or, for example, optical fibers the effect of radiation mainly manifests in a generation of color-centers. At those optical active centers light will be absorbed leading to a loss of transmission. This effect is well known and established ways of testing exist. The parameter dependencies, such as wavelength of transmission, dose, dose rate, temperature, and material properties are known and can be used to define optimized test conditions and find suitable products and operation conditions [2]. Because the radiation-induced attenuation depends linearly on the transmission length, very thin layers of some µm or even nm are usually not strongly affected by this effect.

* jochen.kuhnhenn@int.fraunhofer.de, +49-2251-18200, http://www.int.fraunhofer.de/neo

Further effects in optical materials observed under radiation are compaction or change of refractive index. For example, this can be observed in Fiber-Bragg-Gratings as a shift in their characteristic wavelength. In other media this effect usually is only observed at rather high dose values not common inside of a spacecraft. In other environments than space where high peak dose rates might be present, also the generation of light due to interaction of the radiation can influence signal-to-noise properties or generate transients.

In contrast to the above mentioned effects of larger optical components inside of a space craft, thin coatings facing space suffer additional degradation. Proton irradiation leads to sputtering of atoms from the surface. Depending on orientation or local shielding this can alter the roughness and change the optical properties noticeable. The sputtering efficiency increases with decreasing energy. For 1 keV protons hitting oxygen in a surface SiO_2 layer, more than 3% of the incident particles yield a sputtered atom. In combination with the high number of particles present in space this can lead to degradation.

While the displacement of atoms in bulk materials only leads to a small change of refractive index due to, e.g. compaction, this could be different at the interface of thin layers. Here the displaced atom can be moved into the next layer. The introduction of previously not present elements might change the contrast of refractive index between the layers significantly.

Generally, radiation might also weaken the structural properties of coatings. The mechanical stability under thermal cycling could be reduced after exposition to radiation. Additionally, protons of a particular energy could be accumulated at layer interfaces and form small hydrogen “bubbles” which could trigger blistering of surfaces, especially in combination with temperature variation [3].

Considering those various effects caused by radiation in coatings facing space and not present in conventional optical components, it is obvious that investigation of those effects requires different test designs.

1.2 Space environment relevant for optical coatings

Modelling the space environment and calculating the expected dose and fluence is the first step in any radiation qualification campaign. Over the last decades a set of reliable and accepted models and tools has been developed to determine the radiation limits for components inside of a spacecraft. Since all considered components here are shielded by at least a minimal layer of passive material only particles with energies above a threshold value need to be considered. As a consequence the most common models have rather high cut-off energy, e.g.AP8 or AP9 without the SPM extension start at about 100 keV and AE8/AE9 at 40 keV, ignoring any contribution from particles below that energy.

However, optical coatings without any shielding will get exposed also to these particles and need to be considered. In SiO_2 the range of 100 keV protons is about 1 µm, which could be more than several functional layers of the coating. For 40 keV electrons the range in SiO_2 is even about 14 µm with a mean range around 6 µm. For that reason the models with limited energy range are not suited very well for layers with thicknesses in the 100s of nanometer range.

The composition of the particle energy spectra strongly depends on the orbit. While protons dominate in lower orbits, there are more electrons in the geostationary orbit. Depending on the mission parameters, such as eccentricity, inclination, or time relative to the solar cycle the actual dose and fluence levels differ by orders of magnitude.

Therefore, the analysis of potential effects in optical coatings has to be done on the basis of a relevant radiation environment.

2. INTERACTION OF SPACE RADIATION WITH THIN COATINGS

2.1 Models for estimation of proton and electron spectra

Two example missions are chosen to generate environmental energy spectra of electrons and protons impacting on the layers: one mission in geostationary orbit (GEO) and one mission in Low Earth Orbit (LEO) at 800 km altitude and 98.6° inclination. To better compare the dose levels in these two missions, both missions span 15 years starting 2020-01-01.

The Space Environment Information System (SPENVIS) [4] is used to generate the orbits and the particle spectra. The applied models within SPENVIS are chosen according to the relevant European ECSS standard [5], i.e. AP-8 at minimal solar activity for protons and AE-8 at maximum solar activity or IGE2006 for electrons in LEO or GEO, respectively. Solar protons were modeled with the ESP model at 95% confidence level.

The lower energy range of the AP-8 and ESP models is limited to 100 keV and 40 keV for AE-8, neglecting any particle contributions at lower energies. Simulation results of total in-orbit dose will be limited due to the energy range of these models. The IGE2006 model features an extended electron energy range down to 0.9 keV.

2.2 Range of electrons and protons depending on energy

To evaluate the effects of particles with a given energy, the range of those particles already defines which layers of a coating system could be affected. There exist several methods to determine the average range, also depending on its definition. A common value used is the Continuous Slowing Down Approximation (CSDA) range. It's being calculated by assuming the slowing down at any position along the trajectory to be the total stopping power. If the stopping power is known as a function of energy, the CSDA range can be calculated. This value does not consider any energy straggling or other fluctuations.

For many elements and material mixes the CSDA range can be obtained from estar and pstar, made available by the National Institute of Standards and Technology NIST [5]. The ranges are there given in g/cm², so division by the material density in g/cm³ yields centimeters.

The following Table 1 and Table 2 show the CSDA ranges in µm as tabulated by estar for electrons and pstar for protons for a selection of materials.

Table 1: CSDA ranges in µm for electrons in different materials from estar.

Material	10 keV	50 keV	100 keV	500 keV	1000 keV
Mg	1.95	31.8	104	1256	3080
Si	1.49	24.1	78.5	946	2321
Al	1.31	21.2	69.3	837	2054
SiO_2	1.23	20.2	66.2	801	1971
Ti	0.91	14.3	46.3	550	1345
Ag	0.53	7.6	23.9	274	657
Ni	0.49	7.4	23.8	281	683
Au	0.41	5.1	15.8	172	402

Table 2: CSDA ranges in µm for protons in different materials from pstar.

Material	10 keV	50 keV	100 keV	500 keV	1000 keV
Si	0.23	0.59	0.99	6.20	16.5
Al	0.22	0.58	0.97	5.57	14.6
SiO_2	0.23	0.61	0.97	4.89	13.2
Ti	0.21	0.51	0.80	4.04	10.6
Al_2O_3	0.18	0.47	0.74	3.59	9.32
Ag	0.18	0.45	0.71	3.08	7.34
Au	0.20	0.50	0.75	2.83	6.46

From these two tables already some conclusions can be drawn: The dependence on the material is more prominent for electrons already at lower energies. For protons the range does not differ strongly up to 100 keV. So for protons the energy to reach a certain depth up to 500 nm can be selected around 50 keV. For electrons the range varies strongly with the material. Here the selected penetration of a certain layer requires the knowledge of the used materials. Those tables are useful for first estimations, but lack of precision.

In sophisticated simulations using Monte-Carlo techniques, a more detailed analysis of complex layer structures is possible. As an example we consider an exemplary coating. On a Si substrate (simulated in the following with a thickness of 1 mm), a 50 nm layer of Cr is followed by a 150 nm layer of silver, and finally covered by 120 nm of Al_2O_3. This layer structure is called "protected silver" in the rest of the paper.

In such an example the Monte-Carlo tool SRIM-2013 [7] can be used to calculate the mean range of protons, which is shown in Figure 1. From that analysis we can conclude at which energy the protons are stopping at interfaces within the structure. In this case protons of 15 keV are accumulated between the aluminum oxide and the silver layer. At 48 keV most of the protons stop at the second interface and finally at 58 keV they stop at the substrate interface.

If the accumulation of protons at the interfaces of a layer structure and a potential blistering is in the focus of characterization those energies should be used. If, on the other hand, the damage within the layers is the major concern, proton energies of 6, 35, and 53 keV should be used. Any proton with energies above 65 keV will deposit most of their dose in the substrate and might not be representative for the real environment.

It should be noted that the results shown in Figure 1 are mean ranges, also considering energy fluctuations and scattering, whereas the values in the table above are simpler approximations of the maximum range. As a consequence the values depicted in Figure 1 are lower than the comparable entries in the tables above.

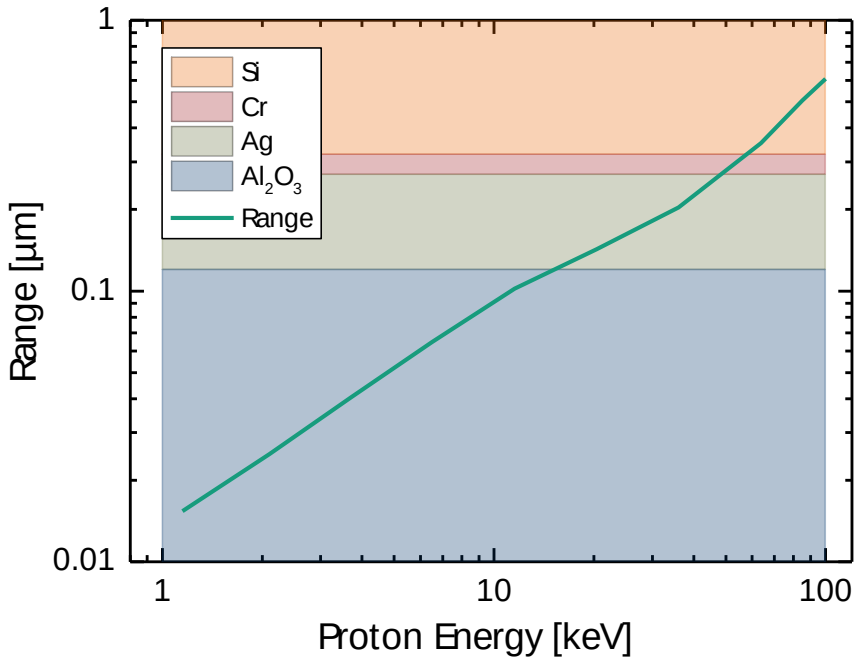

Figure 1. Projected range of protons in protected silver as a function of energy.

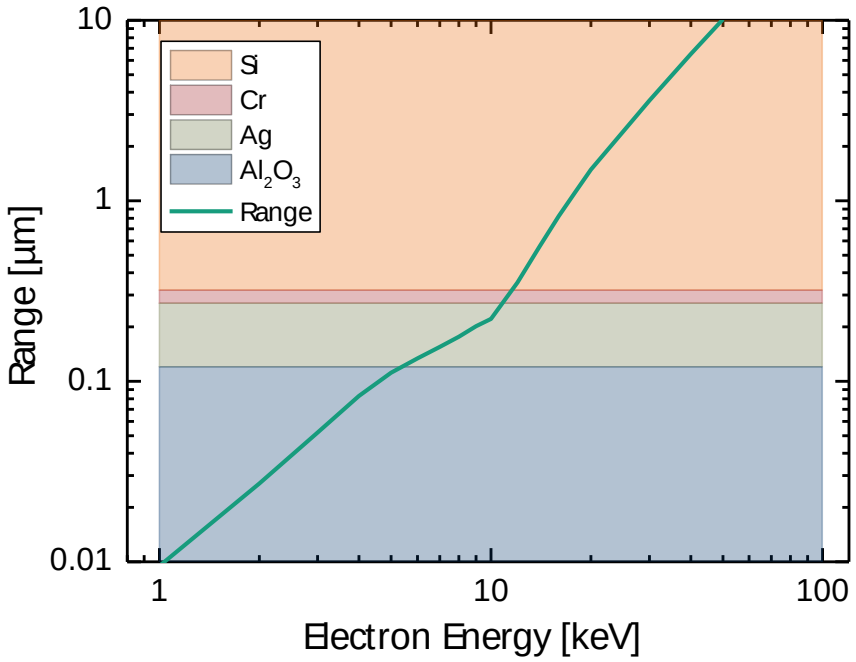

Figure 2. Projected range of electrons in protected silver as a function of energy.

Similar calculations for electrons can be performed with the Monte-Carlo software CASINO [8], as shown in Figure 2. Here also the numerical simulations yield lower ranges. The kink around 10 keV is due to the energy binning of the simulation and the different stopping powers of the materials. The change in slope of the range curve in fact happens at the interface between the silver and chrome layers. A dedicated simulation with higher resolution at this interface depth would be needed to obtain a precise range here.

3. DOSE VALUES IN THIN COATINGS FOR DIFFERENT ORBITS

Several tools were developed to calculate the dose in satellite components in space environments. The main application of those simulations is the definition of radiation levels for electronic components inside a space craft, shielded from the low energy component of space radiation. MULASSIS is one of the tools using Monte-Carlo techniques and is based on the Geant4-framework [9]. Other products widely used are FastRad, Shielddose2 or GRAS.

In this section we consider two example layer systems. The first one, called “protected silver” was already defined above. Additionally a second example “VUV-reflector” is introduced in Table 3.

Table 3: Example layer systems.

	VUV Reflector		**Protected Silver**	
Layer	**Material**	**Thickness [µm]**	**Material**	**Thickness [µm]**
1	MgF_2	0.03	Al_2O_3	0.12
2	Al	0.07	Ag	0.15
3	Si (Substrate)	1000	Cr	0.05
4			Si (Substrate)	1000

For these two layer systems the doses in the respective layers were simulated for two orbits as given in Table 4.

Table 4: Example orbit parameters.

Parameter	Heliosynchronus (LEO)	Geostationary (GEO)
Apogee:	800.00 km	35793.23 km
Perigee:	800.00 km	35793.23 km
Inclination:	98.60°	0.00°
R. A. Ascending Node:	99.74°	99.22°
Argument of Perigee:	0.00°	0.00°
True Anomaly:	0.00°	0.00°
Period:	1.68 hrs	23.93 hrs
Number of orbits:	20	1
Duration:	1.40 days	1.00 days
Orbit start:	01/01/2020 00:00: 0.0	01/01/2020 00:00: 0.0
Orbit end:	02/01/2020 09:37:28.6	01/01/2020 23:56: 4.0
Segment end:	28/12/2034 00:00: 0.0	28/12/2034 00:00: 0.0
Segment length:	5475.00 days	5475.00 days

According to the ECSS standard describing “Particle and UV radiation testing for space materials” [10] this input was used in MULASSIS to calculate dose values as defined in the respective ECSS standard [5]. The software calculates the doses originating from trapped protons, trapped electrons and solar protons. To account for the layer dimensions, all secondary particles with ranges > 1 nm were considered. The following table sums up those contributions in rad per layer.

Table 5: Dose estimations in rad calculated with MULASSIS with standard options.

Protected Silver	LEO	GEO
Al_2O_3	2.2E+07	6.8E+10
Ag	1.3E+07	1.6E+10
Cr	1.7E+07	1.2E+10
Si substrate	7.3E+05	4.9E+07
VUV-Reflector	**LEO**	**GEO**
MgF_2	2.4E+07	1.1E+11
Al	2.1E+07	6.2E+10
Si Substrate	7.5E+05	7.0E+07

This table shows that the first thin layers of the structures facing space receive the highest doses compared to the substrate. That is to be explained by the fact, that only particles of a certain energy can deposit their energy in the lower layers, while particles of lower energy will be stopped in or near the thin layers.

It can also be seen, that in GEO the calculated doses are much higher than in LEO. Two effects are responsible for this: First the number of particles in GEO hitting the coating is much higher than in a quite low orbit. But this enhanced by the

models used to calculate the dose values: for GEO orbits the IGE2006 model uses electron spectra with lower cut-off energy and these low-energy electrons contribute to the dose. In consequence this shows that the results strongly depend on the models used.

For more realistic results models have to be used that include protons and electrons with sufficiently low energies.

How such spectra are absorbed in the example structure is shown in the following figures. Here the incorporation of additional contributions from low energetic particles in MULASSIS clearly shows how the doses are deposited in the different layers.

Comparing Figure 3 and Figure 5 shows how the different first layer thickness protects the remaining structure. While the second layer in the VUV-reflector receives dose from protons of all energies. For the protected silver only protons above 20 keV contribute to the second layer.

This is similar for the dose per electron shown in Figure 4 and Figure 6. In both examples the proton deposition curves exhibit a kink around 1 MeV incident energy in the substrate. This is probably caused by the codes of the simulation. Comparable calculations with GRAS show the same pattern.

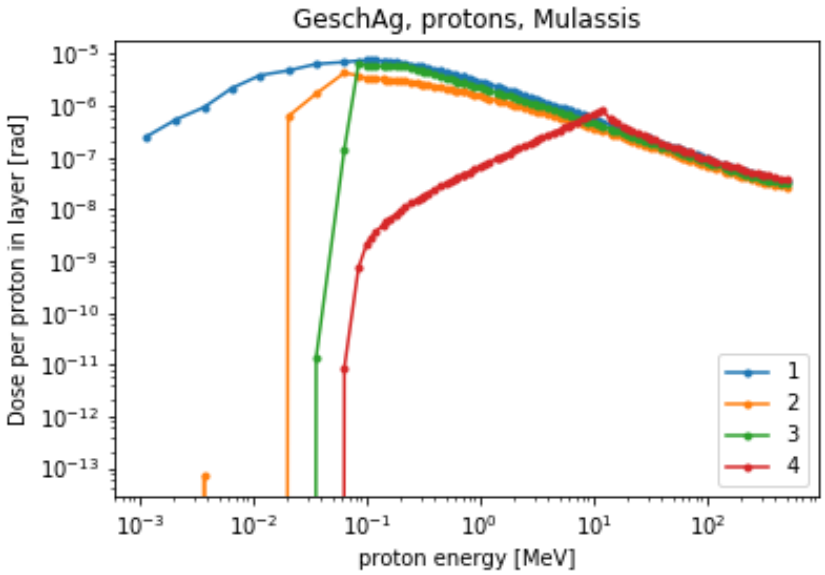

Figure 3. Dose per proton in protected silver. Layers according to Table 3.

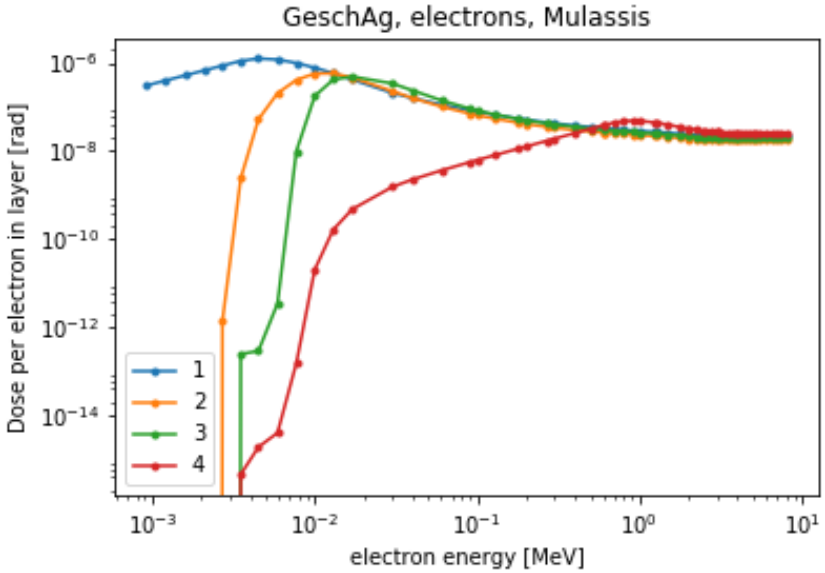

Figure 4. Dose per electron in protected silver. Layers according to Table 3.

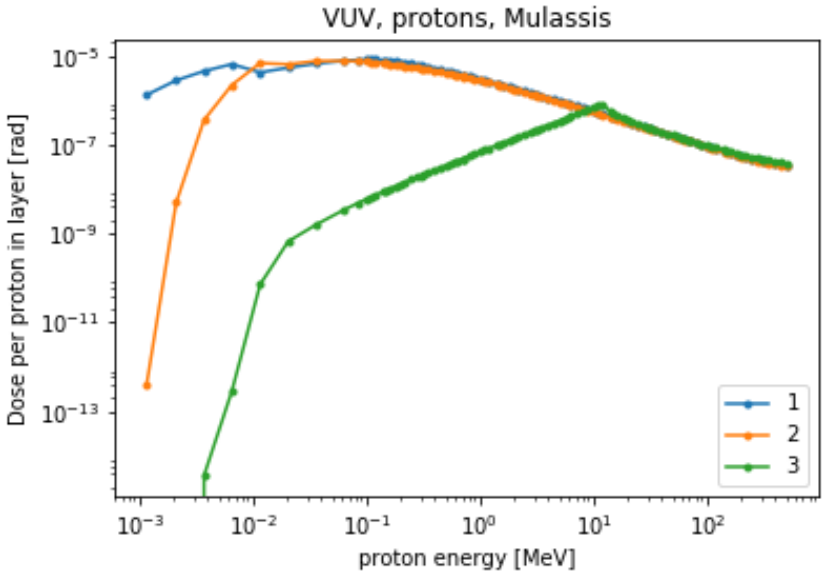

Figure 5. Dose per proton in VUV-reflector. Layers according to Table 3.

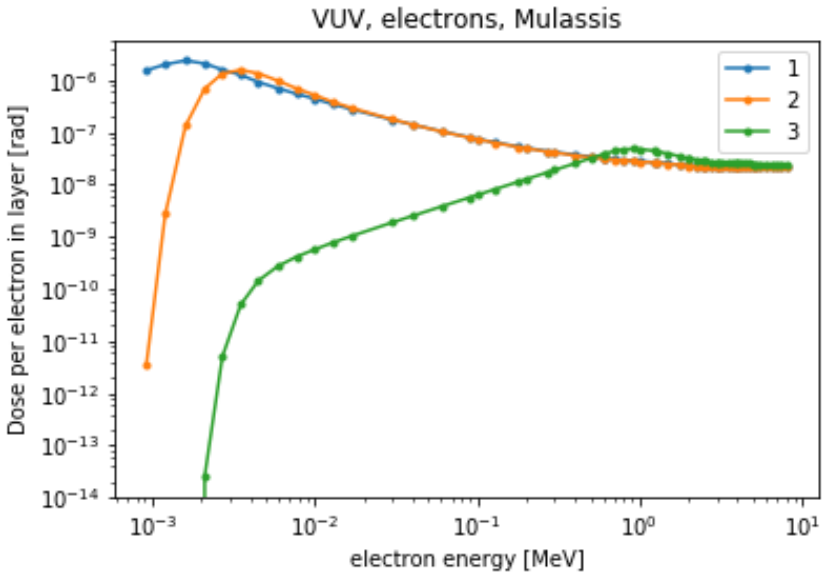

Figure 6. Dose per electron in VUV-reflector. Layers according to Table 3.

4. SIGNIFICANCE FOR RADIATION TESTING

The examples above have shown that the determination of doses in thin layers of an optical coating is strongly depending on the input parameters, especially the used particle spectra. Secondly the structure of the layer system changes the dose deposition depending on thickness and material. From that is obvious that any realistic radiation test has to optimize the test parameters regarding particle type and energy used.

Testing with Co-60 gamma photons will not reproduce the dose depth profile of thin layers facing space. Due to the high energy, the photons will release their energy along their path through the samples uniformly. The substrate will receive a similar dose than the first layer, which will dramatically overtest the substrate if one uses the dose value calculated for this first layer, or will not get close to realistic exposition if only the substrate value is used.

Another source for misleading test parameters is the fact that at low energies the particles might stop within the first layer, depositing all their energy within the first 100 nm, for example. Under those conditions the thickness of the layer will reduce the calculated dose, because of its larger mass. But the first 100 nm will still receive the same damage.

Radiation testing of thin coatings cannot be done with a fixed set of particles and energies. To adequately design a radiation test procedure of the following chapters is suggested.

4.1 Definition of layer structure

As shown above all simulations are only valid for defined layer materials and thicknesses. So for any application the structure of the coating needs to be static. Depending on the simulation results a change of design can be useful, for example, to have a thicker layer of protection. What should be kept in mind, is that for thin deposited layers, the density, which is a crucial factor in the simulations, might be different from the usual tabulated bulk properties.

4.2 Determination of ranges

Next the ranges of electrons and protons are calculated within the structure with Monte-Carlo codes, such as SRIM or CASINO. A set of energies between, e.g. 1 keV and 1 MeV should be used to obtain critical energies, i.e. at which energy the particles are stopping at interfaces and at which energies particles will penetrate functional layers.

4.3 Selection of relevant environment model

Depending on the ranges and critical energies a suitable environment model has to be used, providing particle fluxes at least down to the relevant energies. Using this input and the mission orbit parameters, the environment can be calculated. Current models covering low energy particles might exhibit discontinuities that could influence the results.

4.4 Calculation of dose values

Based on the spectra and the structure definition the dose values of the individual layers are calculated. Some codes even provide the dose depth curve of each or all layers. That provides valuable insight of the dose distribution. If possible, several codes should be used to discover systematic discrepancies between them. GRAS and MULASSIS can be used for protons and electrons, SRIM and CASINO are only simulating one particle each.

It should be mentioned, that some numerical codes will ignore secondary particles with lower range. To produce reliable results also for thin layers, this setting should be optimized.

4.5 Definition of particles and energies for radiation testing

Finally a test process can be defined. Typically that will yield a set of mono-energetic beams for protons and electrons. The selection of energy and particle should include some considerations: Define ranges of suitable proton energies to deposit protons at interface depth to reproduce accumulation of hydrogen, define a set of possible proton and electron energies to deposit doses in each layer similar to the application environment, and only then identify facilities with the required energy ranges.

Defining the proton and electron energies beforehand or according to available facilities will not realize a suitable radiation test.

REFERENCES

[1] ISO 15856:2010: Space systems -- Space environment -- Simulation guidelines for radiation exposure of non-metallic materials (2010)
[2] Girard, S., Kuhnhenn, J., Gusarov, A., Brichard, B., Van Uffelen, M., Ouerdane, Y., Marcandella, C. “Radiation effects on silica-based optical fibers: Recent advances and future challenges.” IEEE Transactions on Nuclear Science, 60(3), 2015-2036. (2013). DOI: 10.1109/TNS.2012.2235464
[3] Liu, H., Hongbin, G., Yang, D., Abramov, V. V., & Wang, H. “Effects of space environment factors on optical materials.” Journal of spacecraft and rockets, 42(6), 1066-1069. (2005). DOI: 10.2514/1.20885
[4] Space Environment Information System (SPENVIS), https://www.spenvis.oma.be , (accessed 2018)
[5] ECSS-E-ST-10-04C, “Space Engeneering – Space Envirnment.”, http://ecss.nl/standard/ecss-e-st-10-04c-space-environment/, (2008).
[6] Berger, M.J. et al., Stopping-Power & Range Tables for Electrons, Protons, and Helium Ions, NIST Standard Reference Database 124. (2017). DOI: 10.18434/T4NC7P
[7] Ziegler, J: “The Stopping and Range of Ions in Matter.” SRIM 2013. http://www.srim.org/. (accessed 2018)
[8] Drouin, D.: “monte CArlo SImulation of electroN trajectory in sOlids.” http://www.gel.usherbrooke.ca/casino/. (accessed 2018)
[9] Lei, F., Truscott, R. R., Dyer, C. S., Quaghebeur, B., Heynderickx, D., Nieminen, R., Daly, E.. MULASSIS: A Geant4-based multilayered shielding simulation tool. IEEE Transactions on Nuclear Science, 49(6), 2788-2793. (2002) DOI: 10.1109/TNS.2002.805351
[10] ECSS-Q-ST-70-06C, “Space product assurance – Particle and UV radiation testing for space materials”. http://ecss.nl/standard/ecss-q-st-70-06c-particle-and-uv-radiation-testing-for-space-materials/ (2008)